

THE SINGLE-BEAM FUNNEL DEMONSTRATION: EXPERIMENT AND SIMULATION *

K. F. Johnson, O. R. Sander, G. O. Bolme, J. D. Gilpatrick, F. W. Guy,
 J. H. Marquardt, K. Saadatmand,** D. Sandoval, and V. Yuan
 Los Alamos National Laboratory, Los Alamos, NM 87545

ABSTRACT

Accelerator concepts for heavy-ion fusion and for the transmutation of nuclear waste require small-emittance, high-current beams. Such applications include funnels in which high-current, like-charged particle beams are interlaced to double the beam current. The first experimental demonstration confirming the beam dynamics of the funnel principle (with contained emittance growth) was recently completed at Los Alamos National Laboratory. A single leg of a prototype 5-MeV, H⁻ funnel was successfully tested. This single-beam demonstration explored physics issues of a two-beam funnel. The experiment contained elements for emittance control, position control, and rf-deflection. Diagnostics allowed measurement of beam intensity, position and angle centroids, energy and phase centroids, transverse and longitudinal phase-space distributions. Results of the experiment will be presented along with comparisons to simulations.

INTRODUCTION

An experimental demonstration confirming the beam dynamics of beam funnelling was recently completed on the Accelerator Test Stand (ATS)¹ at Los Alamos National Laboratory. Although this experiment utilized a single-leg of a prototype 5-MeV H⁻ funnel, it addressed most of the physics issues concerned with a two-beam funnel. The only known beam dynamics issue that was not addressed was the beam-beam interaction. Objectives of this experiment were position control (with ~100% beam transmission), successful use of rf-deflection,³ and control of emittance growth.

EXPERIMENTAL TECHNIQUE

The H⁻ input beam was from the ATS, 425-MHz, 5-MeV drift tube linac (DTL). The beamline is shown schematically in Fig. 1. Beam position control was achieved with four permanent-magnet dipoles (PMDs), four off-set permanent-magnet quadrupoles (PMQs), four movable PMQs for steering, and one rf deflector. Reference 2 contains component design specifications for the funnel beamline. Funnel transverse emittance control was maintained by 15 PMQs. The PMQ focusing was chosen to match the periodic focusing of the ATS DTL. Funnel longitudinal emittance control was done with four rf bunchers (two 425-MHz and two 850-MHz), whose amplitude and phase could be independently varied to change the longitudinal emittance shape.

Beamline diagnostics included three broad-band toroids and nine microstrip probes (MBPs). A large cylindrical vacuum vessel contained the beamline which was mounted on four separate plates (M1 through M4) to allow for staged installation (Fig. 1). The diagnostics for beam characterization were mounted on a diagnostics plate (D-plate), which was placed after each M-plate. The diagnostics consisted of two pairs of slit-collectors for transverse emittance measurements, the LINDA³ (a longitudinal emittance measurement technique) intersection points and a sweeping

magnet for longitudinal emittance measurements, three MBPs, one wide-band toroid, a beam stop, and a Faraday cup.

EXPERIMENTS AND RESULTS

The single-beam funnel experiment was performed in four stages. They were the characterizations of the output beams from the DTL, M1-, M3- and M4-plates.

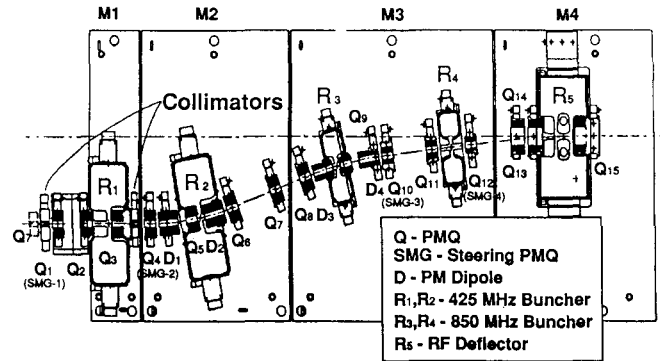


Fig. 1. Funnel beamline schematic. Shown are the locations of the optics elements. These included PMQs (fixed and movable), PMDs, collimators, and rf cavities.

Characterization of the DTL

The DTL rf amplitude and phase set-points were determined using the phase-scan technique.^{4,5} This technique utilizes MBPs to measure the energy and phase centroids of the beam as a function of the DTL amplitude and phase. A comparison of data to single-particle simulations provides the signature for determining the DTL operating set-points. The phase-scan hardware-software system allows rapid determination of the DTL set-points (5 to 10 minutes). The rf amplitude was also determined by monitoring high-energy x-rays⁶ from the DTL. Disagreement in the determination of the DTL gap voltage from phase-scan or x-ray data was ≤5%.

Longitudinal and transverse phase-space distributions were characterized as a function of DTL amplitude and phase. Comparisons between these measurements and those made previously indicated a problem with respect to the transverse phase-space. The transverse emittance in the horizontal and vertical planes had increased by a factor of 1.7 to 2.0 over the previously observed values. Extensive instrumental checks showed that the increase was real. Scheduling constraints limited the search for the cause of this emittance growth, so an alternative approach was used. Two collimators (movable vertically and horizontally) were installed on the M1-plate (at its entrance and exit). The collimators were designed to reduce the transverse emittance to an acceptable level to permit a meaningful physics test of the remainder of the funnel beamline (i.e., the M2- through M4-plates).

Characterization of the M1-Plate

The M1-plate contained one 425-MHz buncher cavity (R1), one movable and two fixed PMQs, three MBPs, one toroid, and two movable collimators. The positions of the

*Work supported and funded by the US Department of Defense, Army Strategic Defense Command, under the auspices of the US Department of Energy.

**Industrial partner, Grumman Corporate Research Center.

movable collimators and movable PMQ (SMG1) were optimized to prepare the beam for injection into the M2-plate. The final settings of the collimators and SMG1 were fixed for the duration of the funnel experiment. The M1-plate beam transmission was ~58%. Depending on ATS operation, the M1-plate output current varied from 25 to 40 mA.

Phase-scans were made to determine the R1 rf amplitude and phase set-points. With the collimators and R1 set, the transverse and longitudinal phase-spaces of the collimated beam were characterized. The expected transverse emittance was achieved (~0.021 π cm-mr in each plane).

Characterization of the M2- and M3-Plates

The M2- and M3-plates contained nine PMQs (three movable), three rf bunchers (one 425-MHz, R2, and two 850-MHz cavities, R3 and R4), four PMDs, six MBPs, and two broad-band toroids.

Good transmission (~100%) through the M2- and M3-plates was achieved with the steering PMQs (SMG2-SMG4). These PMQs were used to adjust the beam position and angle centroids for injection into the M4-plate. The error on the transmission measurement was dominated by beam noise and not toroid measurement precision. For quiet beams, a relative uncertainty of ~2% on beam transmission was possible.

The funnel steering model was checked by moving the SMGs one at a time, vertically or horizontally, and measuring the changes in beam position and angle centroids at the funnel exit. In general, the model and measurement agreed within the experimental errors of ± 0.2 mm and ± 1 mr.

The phase set-points for R2, R3, and R4 were determined by beam loading and the amplitude set-points were determined by using LINDA to measure beam energy gain. The phase-scan technique could not be used due to RFI (rf interference) in the MBPs. The RFI significantly reduced the accuracy of the microstrip measurements of position, angle, energy, and phase centroids. The principal source of the RFI was rf leakage from the R1 cavity and the beam itself.

Longitudinal and transverse phase-space distributions were measured for optimum settings of the four rf bunchers. To study phase-space distribution sensitivities to non-optimum conditions, the measurements were repeated as conditions were adjusted (all rf buncher amplitudes decreased by 20%, all rf bunchers off, etc.). The normalized horizontal (vertical) transverse emittance ϵ_x (ϵ_y) was unchanged when the buncher amplitudes were decreased by 20% from their optimum settings. For bunchers off, ϵ_x increased by ~33% (dispersion in the bend plane), but ϵ_y remained unchanged, as expected.

Characterization of the M4-Plate

The M4-plate contained three PMQs, the rf deflector (425-MHz), two MBPs, and one toroid. The D-plate was aligned with the deflector "on" beam axis. This choice prohibited certain types of measurements when the deflector was "off."

Good transmission (~100%, 2% relative uncertainty) was achieved through the rf deflector with rf power "on" or "off." To achieve this level of transmission, slight adjustments of SMG2, SMG3, and SMG4 were necessary.

RF deflector performance was critical to the success of the funnel experiment. The horizontal beam deflection, the relative ϵ_x and ϵ_y , and ϵ_L were measured as functions of deflector phase and cavity power. The rf power set-point was determined from x-ray monitor data. For 86 kW of cavity rf power, analysis of the x-ray data gave a gap voltage of 333 ± 17 kV (design value 333 kV). Figures 2 and 3 show the dependence of the relative horizontal beam deflection and relative ϵ_x on the relative deflector phase. Both the deflection and ϵ_x show extremums at the same input phase. This behavior is also observed for the Courant-Snyder parameters α , β , and γ . The extremums in β and γ are related to minimization of position and angle spreads. There is a clear signature for the rf phase set-point (~60° relative phase) of the deflector. This phase was shown to be independent of cavity power (Fig. 2), and ϵ_y was shown to be independent of the deflector phase. Both observations were as predicted. The behavior of ϵ_L with respect to deflector phase (Fig. 4) is similar to that of ϵ_x . Although broader, its minimum occurs at approximately the same phase, as it should.

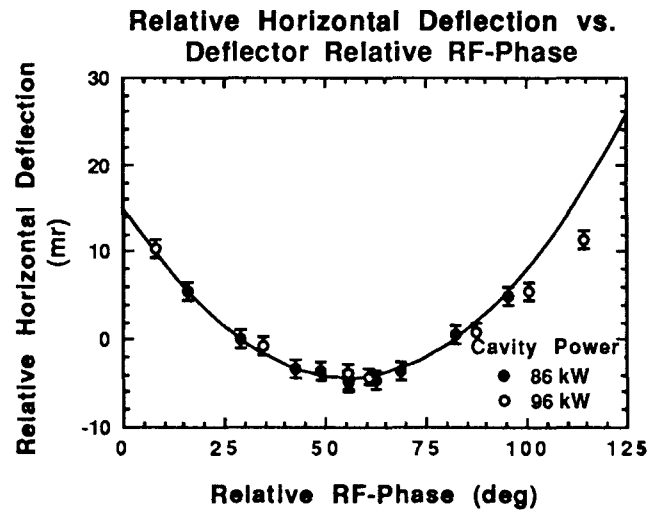


Fig. 2. Relative deflection angle of the deflector output beam in the horizontal (bend) plane vs. relative deflector phase. Data are shown for two deflector cavity power levels. The curve is to guide the eye.

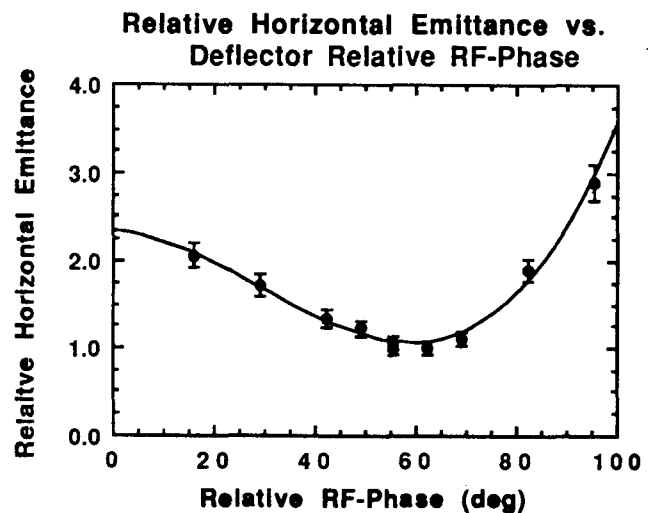


Fig. 3. Relative ϵ_x of the deflector output beam in the horizontal plane vs. relative deflector rf phase. Cavity power set at 86 kW. The curve is to guide the eye.

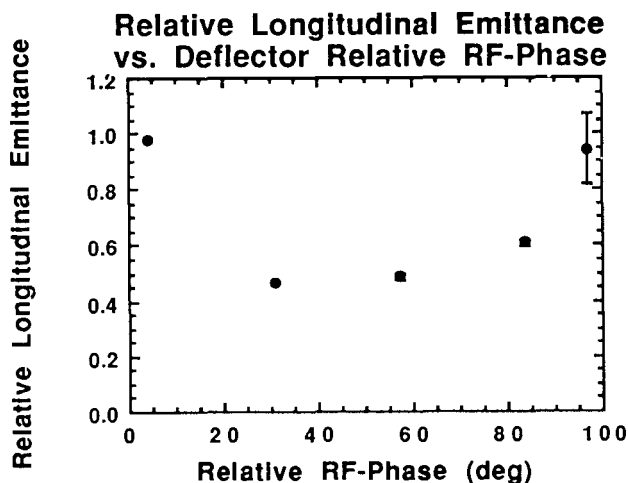


Fig. 4. Relative ϵ_L vs. relative deflector phase. Deflector cavity power set at 86 kW.

Relative ϵ_x , ϵ_y , ϵ_L , and the Courant-Snyder parameters (in x and y) were shown to be independent of deflector cavity power.

With the rf deflector set at its experimentally determined "best" power and phase set-points, the measured absolute horizontal deflection of the beam was 36 ± 2 mr. Simulations predicted a deflection of 38.4 mr. Within the experimental error (± 2 mr) and the 5% uncertainty in gap voltage, there was excellent agreement between measurement and simulations. The beam deflection scaled with rf power as expected.

With the four bunchers and the rf deflector at their optimum phase and amplitude set-points, the transverse and longitudinal phase-space distributions were measured. When the observed emittances and currents at the exit of the M1-plate are used as input, simulations predict an upper limit of ~5% transverse emittance growth through the rest of the funnel beamline. Within experimental error, the data ($\epsilon_x = 0.022 \pi$ cm-mr or $\epsilon_y = 0.020 \pi$ cm-mr) are consistent with simulations and with no transverse emittance growth. The short-term and day-to-day reproducibility of the data is 2 to 3% and 8 to 10%, respectively. The error on the emittance measurements is 5 to 8% with background subtraction being the dominant component of the error.

The attempt to produce a measureable emittance growth with non-optimum operation of the rf bunchers (amplitudes 20% low) also produced a null result (consistent with simulations). With the four rf bunchers "off", ϵ_x increased by ~33%, at the M3-exit, and by a factor of 3 at the M4-exit (due to beam debunching). Large emittance growth (in ϵ_x and ϵ_L) was also observed for improper phasing of the deflector (Figs. 3 and 4).

Using the DTL design ϵ_L as input, simulations predict an upper limit of ~5% ϵ_L growth through the funnel. The observed growth was ~15 to 20%. The error on ϵ_L is a few percent (~5%) and reflects the scatter in the measured values. The results for non-optimum buncher operation were basically the same. The measured ϵ_L of the DTL output beam was ~4 times smaller than the design value of ϵ_L , so even a 20% emittance growth through the funnel was not detrimental to the funnel's performance.

SUMMARY OF THE FUNNEL PERFORMANCE

The major objectives of the ATS single-beam funnel were realized. Position (i.e., steering) control was achieved throughout the funnel with a ~100% beam transmission.

The use of rf-deflection was successful. The dependence of beam deflection, ϵ_x and ϵ_y , the horizontal Courant-Snyder parameters, and ϵ_L on deflector amplitude and phase was as expected. The desired amplitude and phase set-points were easily determined.

Transverse and longitudinal emittance growth through the ATS single-beam funnel were controlled. Within experimental precision no transverse emittance growth was observed as expected. Non-optimum operation of the rf bunchers also failed to produce any measureable transverse emittance growth.

Longitudinal emittance growth through the ATS single-beam funnel was controlled to a level which was not detrimental to the funnel's performance. A measurement of longitudinal emittance growth in a drift (~35 cm) showed large growth (60-80%). Transverse and longitudinal emittance control in the funnel beamline (length ~160 cm) has eliminated this large growth.

ACKNOWLEDGEMENTS

The successful completion of the ATS single-beam funnel experiment would not have been possible without the cooperation of many individuals throughout the Accelerator Technology Division of LANL.

REFERENCES

1. O. R. Sander, et al., "Review of the Accelerator Test Stand Performance and Expectations," 1989 Neutral Particle Beam Technology Symposium, Monterey, CA, July 1989.
2. R. J. Kashuba, et al., "Physics Design of the ATS Funnel Experiment," 1989 Neutral Particle Beam Technology Symposium, Monterey, CA, July 1989.
3. W. B. Cottingham, et al., "Noninterceptive Technique for the Measurement of Longitudinal Parameters of Intense H⁺ Beams," Proc. 1985 Particle Accelerator Conference, IEEE Trans. Nucl. Sci. 32 (5), 1871 (1985).
4. C. M. Fortgang, et al., "Longitudinal Beam Dynamics of a 5-MeV DTL," 1988 Linear Accelerator Conference, Williamsburg, Virginia, October 1988, Continuous Electron Beam Accelerator Facility CEBAF-Report-89-001 (June 1989), p. 167.
5. J. D. Gilpatrick, et al., "Synchronous Phase and Energy Measurement System for a 6.7 MeV H⁺ Beam," 1988 Linear Accelerator Conference, Williamsburg, Virginia, October 1988, Continuous Electron Beam Accelerator Facility CEBAF-Report-89-001 (June 1989), p. 134.
6. G. O. Bolme, et al., "Measurement of RF Accelerator Cavity Field Levels at High Power from the Characteristic X-ray Emissions," this conference.